ISSN 3047-5473
Innovation in Engineering, Volume 1, Nomor 2, 2024, pp. 73-95

Static analysis of boiler feed pump shaft in steam power plants: Enhancing durability and operational efficiency

Muhammad Athar Altarisi, Rifelino*, Delima Yanti Sari and Wanda Afnison

Department of Mechanical Engineering, Universitas Negeri Padang, **Indonesia**

*Corresponding Author: rifelino@ft.unp.ac.id

DOI: https://doi.org/10.58712/ie.v1i2.8

Abtract: Centrifugal pumps are commonly used in industrial and domestic sectors to transport fluids by increasing their flow rate to a specific pressure. One type of centrifugal pump, the Boiler Feed Pump (BFP), plays a crucial role in steam power plants. Designed for continuous operation, BFP shafts are prone to wear and failure due to extreme operational conditions. This study employs computer-aided simulation using SolidWorks software to analyze von Mises stress, displacement, strain, and safety factors of BFP shafts with three material variations: AISI 4140, AISI 316, and AISI 304. The results indicate that AISI 4140 material exhibits the highest safety factor of 2.7 and the lowest displacement of 0.453 mm. Fatigue simulation also shows that AISI 4140 has the lowest damage percentage and the highest fatigue life. These findings suggest that AISI 4140 is the optimal material choice to enhance the durability and efficiency of shafts in applications requiring high reliability, such as BFPs in steam power plants.

Keywords: Centrifugal pump; Boiler feed pump; Computer-aided engineering simulation; Material fatigue; Safety factor

1. Introduction

Centrifugal pumps are among the most widely utilized machines in industrial and domestic settings [1], [2]. These turbo-machines are designed to transport liquids by increasing the flow rate to a specific pressure level. They operate on the principle of dynamically accelerating fluids using centrifugal force to convert kinetic energy into pressure [3]. A centrifugal pump comprises mechanical and hydraulic components, with its hydraulic performance significantly influenced by these mechanical parts [4], [5]. This paper focuses on the multistage type of centrifugal pumps [6].

The Boiler Feed Pump (BFP) is a specific type of centrifugal pump that transfers fluids by raising their pressure level [7], [8], [9]. In steam power plants (PLTU), the BFP plays a crucial role and is often regarded as the "heart" of the plant. High-pressure steam drives

Received: June 25, 2024. **Revised**: August 26, 2024. **Accepted**: August 30, 2024

turbines, which rotate generators directly connected to the turbines, generating electricity [10]. This steam is produced by feeding hot water from the Boiler Feed Pump to the boiler [11].

According to R. A. Ufa et al [12], the feedwater system is a critical component of a power generation unit. If the function of the Boiler Feed Pump is compromised, it can negatively impact the power plant's performance. The BFP is designed to continuously supply high-power output steam boilers, providing pressurized water that is converted into electricity. This pump comprises interconnected components that work as an integrated unit, including the shaft, impeller, and balance disk. The shaft, which is the primary component, plays a pivotal role in transmitting rotation from the driving source, such as an electric motor, to the pump components that rely on it [13], [14], [15].

The Boiler Feed Pump is a multistage centrifugal pump featuring several impellers arranged in series within a single casing, all mounted on a shaft supported by bearings on both ends [16], [17]. As a result, the BFP shaft endures greater loads than those in single-impeller centrifugal pumps. Continuous operation of these pumps inevitably leads to wear and potential failures, such as shaft fractures or cracks near bearings or coupling hubs [18]. Boiler feed pump turbines face numerous failures, including high temperatures and vibrations at bearings and mechanical seals, valve and line connection leaks [19], as well as issues related to the coupling between the pump and the gearbox that can cause shaft misalignment [20]. Examples of such failures observed in the field are illustrated in Figure 1.

Figure 1: Damage to the shaft

Figure 1 illustrates visible damage to the shaft, highlighted with a pen and arrow for clarity. Such damage can result in excessive clearance due to dimensional changes, affecting the moving components that rely on the shaft. Consequently, simulation processes are crucial to provide insights into the potential effects on the shaft when subjected to load. SolidWorks software is a suitable method for this purpose, as it allows for visual analysis of von Mises stress, displacement, and the safety factor on the design [21]. The findings from these simulations offer valuable information for further analysis, guiding the necessary actions to improve the durability and efficiency of the shaft.

2. Methods

This study conducted a CAE simulation on the shaft design using three different materials: AISI 4140, AISI 316, and AISI 304. This simulation aims to obtain a comparative analysis of these materials based on their mechanical properties and performance under stress [22], [23]. By assessing factors such as stress distribution, displacement, strain, and fatigue life for each material, the study aims to identify which material offers the optimal combination of strength, durability, and reliability for use in demanding engineering applications. Understanding the material characteristics and their responses under load conditions is crucial for improving the shaft's overall performance and ensuring its longevity in industrial environments [24].

2.1 Shaft design

The shaft was designed using SolidWorks software. Additionally, simulations were conducted utilizing the same application, employing computer-aided engineering simulation methods [25]. This integrated approach allows for precise modelling and analysis of the shaft's performance under various conditions, facilitating an in-depth understanding of its mechanical behaviour and ensuring that design specifications are met effectively.

Figure 2: 3D Shaft Model Design

2.2 Material

In the research, static and fatigue simulations were conducted using three different materials: AISI 4140, AISI 316, and AISI 304. The properties of these materials are detailed in Table 1. This selection of materials allows for a comprehensive evaluation of the shaft's performance under various conditions, facilitating a comparison of their mechanical properties and their impact on the simulation results.

Table 1: Material properties

Property	AISI 4140	AISI 316	AISI 304
Elastic Modulus	205000 N/mm^2	192999 N/mm^2	190000 N/mm^2
Poisson's Ratio	0.29 N/A	0.27 N/A	0.29 N/A
Shear Modulus	80000 N/mm^2	-	75000 N/mm^2
Mass Density	7850 kg/m^3	8000 kg/m^3	8000 kg/m^3
Tensile Strength	814 N/mm^2	580 N/mm^2	517 N/mm^2
Yield Strength	485 MPa	172 MPa	207 MPa

2.3 Defining the pedestal

Prior to conducting the simulations, it is essential to apply support. For the shaft in this study, supports are positioned at the bearing regions, utilizing bearing support types. This setup ensures the shaft is accurately constrained and the simulation results reflect realistic operational conditions. Correctly applying these supports is crucial for accurately assessing the shaft's performance under various loading scenarios and ensuring that the analysis effectively mirrors practical engineering applications presented in Figure 3.

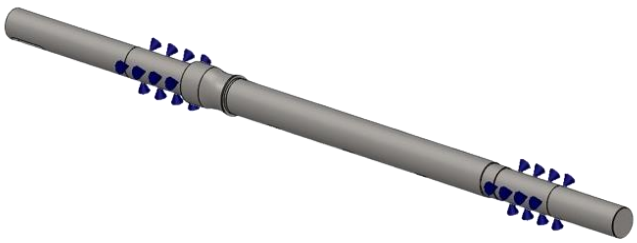

Figure 3: Torque loading on shaft

2.4 External loads

In this study, static load testing was conducted by applying various loads to the shaft design. The magnitude of these loads can be determined using the following formula. The results from these tests are essential for assessing the shaft's performance and ensuring that it meets the required engineering standards for reliability and durability.

$$W = m\ x\ g \tag{1}$$

Impeller Mass = 15.04 kg
= 15.04 kg × 9.81 m/s^2 = 147.5 N
Mass 6 Impeller = 6 × 147.5 N = 885 N
Disk balance mass = 8.42 kg
= 8.42 kg × 9.81 m/s^2 = 82.6 N

$$\tau = \frac{p}{\omega} \tag{2}$$

By using the Eq. 2, the following results are obtained:

P = 560 Kw = 560.000 watt
ω = 2980 Rpm = 312 rad/s

$$\tau = \frac{560.000}{312} = 1.794 \text{ Nm}$$

In order to find out the load area can be seen in Figure 4.

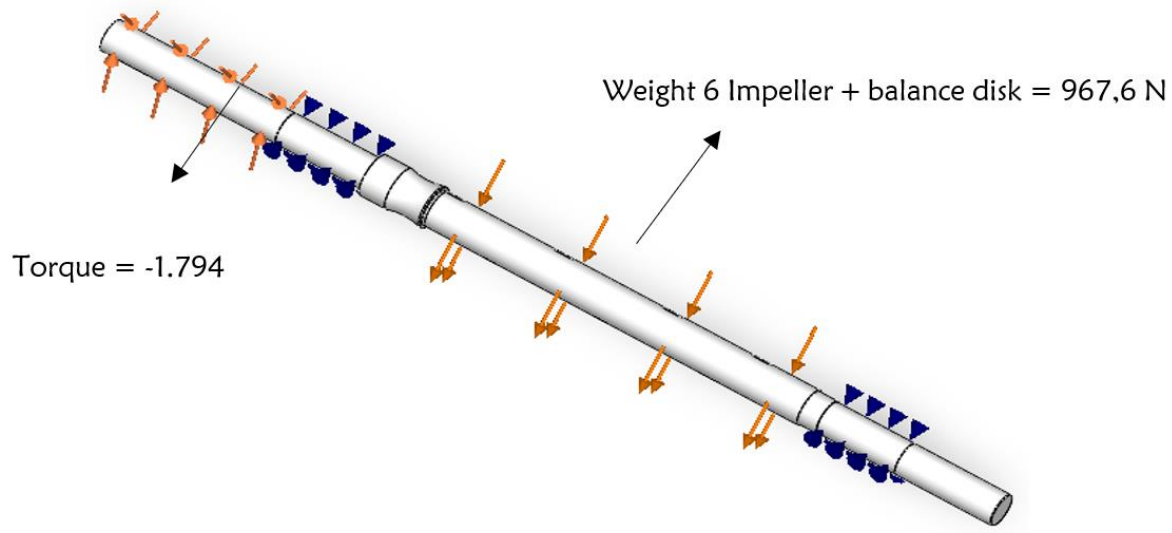

Figure 4: Torque loading on shaft

2.5 Mesh independent test

The purpose of conducting a mesh independence study is to determine the optimal mesh density for use in simulations of the 3D shaft design [26], [27]. Each mesh level will yield different results and require varying computational time. The simulations performed on the 3D shaft model include static and fatigue analyses with varied materials. The comparison of these simulations encompasses stress values, mesh levels, and completion times, illustrated in the graph shown in Figure 4. Results from simulations with different mesh densities indicate variations in stress values and completion times, highlighting the impact of mesh density on the accuracy and efficiency of the simulation.

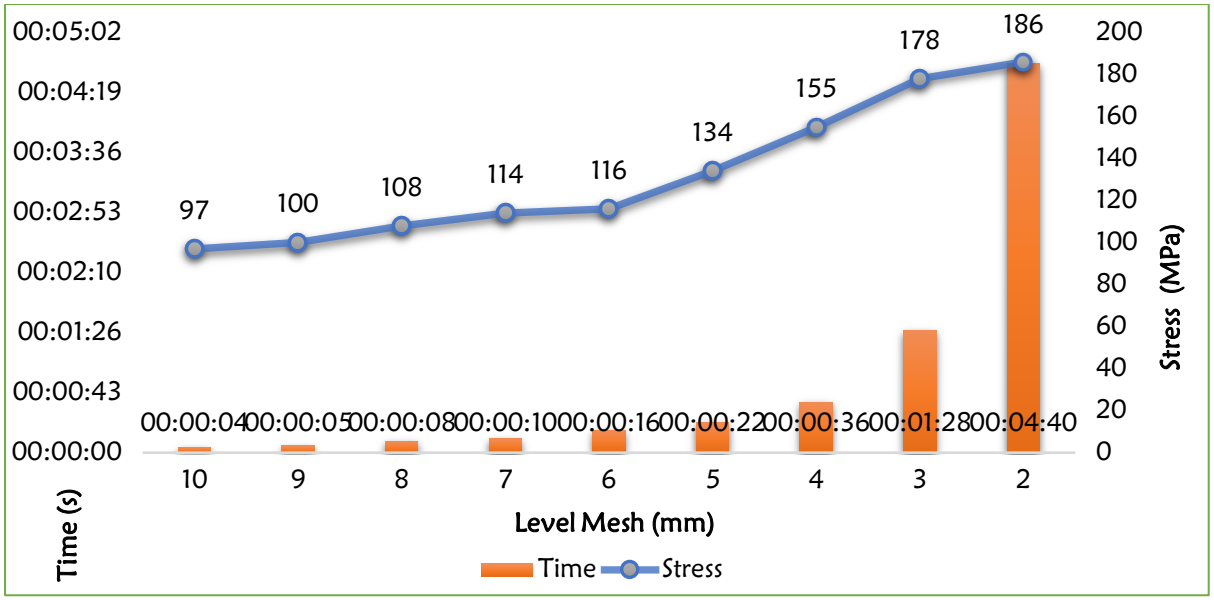

Figure 5: Mesh independence test

As depicted in the simulation results shown in Figure 5, decreasing the mesh level or density increases stress values and extends the completion time. The objective of analyzing Figure 5 was to identify the mesh level that effectively balances accuracy and computational efficiency. The study's findings reveal that as mesh size decreases, the simulation results more closely approximate experimental outcomes [28], [29]. Consequently, the chosen mesh level for this research is Level 3, based on the observation that higher stress values are associated with Mesh Levels 3 and 2, while Mesh Level 2 requires more time to complete than Level 3. Mesh Level 3 yields a stress value of 178 MPa with a completion time of 1 minute and 28 seconds. The meshing results for the shaft are illustrated in Figure 6.

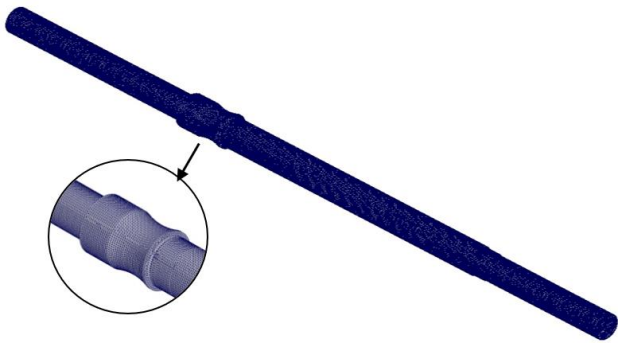

Figure 6: Mesh boundary on shaft

3. Results and discussion

3.1 Static simulation

After completing the static simulations, several outcomes were obtained, including Von Mises stress, displacement, strain, and safety factor. These results provide a

comprehensive assessment of the structural performance of the shaft under static loading conditions. The Von Mises stress indicates the material's ability to withstand applied forces, while displacement measures the extent of deformation. Strain quantifies the material's deformation relative to its original dimensions, and the safety factor assesses the margin by which the design can handle additional loads beyond the anticipated maximum. These metrics are essential for evaluating the shaft' s robustness and reliability.

3.1.1 Stress (Von mises stress)

The results of the static stress simulations conducted on the 3D shaft design, subjected to torsional loads, impeller weights, and balance disk forces using SolidWorks Simulation, reveal that the maximum stress recorded for shafts made of AISI 4140, AISI 316, and AISI 304 materials is 178 MPa. It is important to note that these stress values exceed the elastic limit of the materials, which could lead to structural changes and potential failure [30]. The visual representation of these stress results is shown in Figure 7.

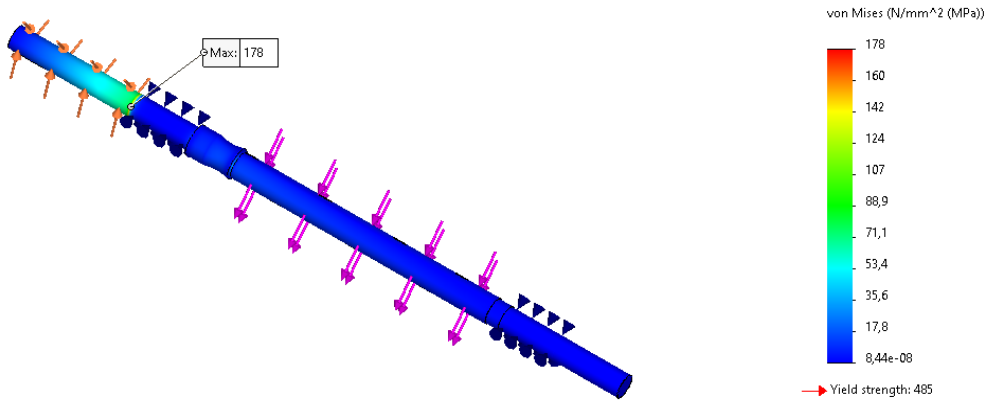

(a)

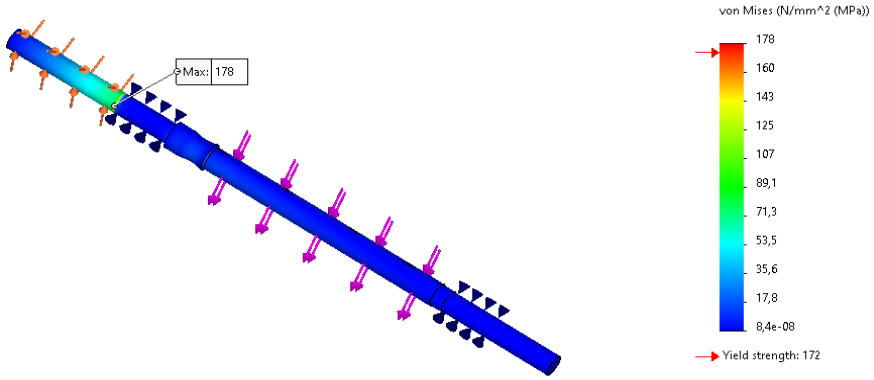

(b)

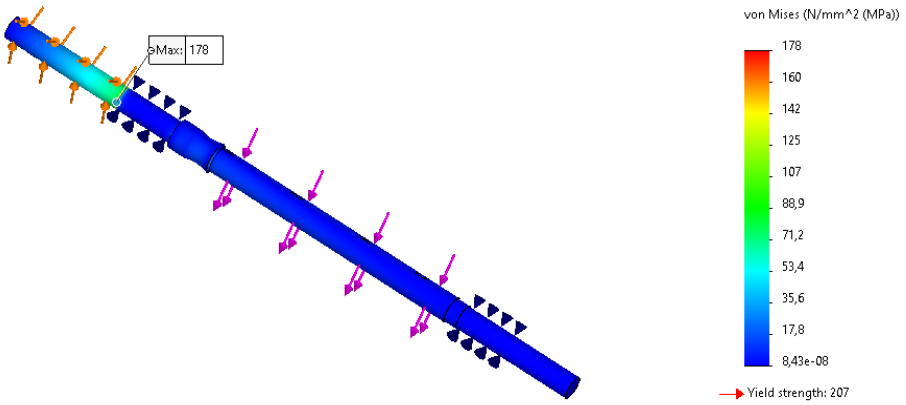

(c)

Figure 7: Shaft stress values (a) Material 4140 (b) Material 316 (c) Material 304

3.1.2 Displacement

The results of the static displacement simulations conducted on the 3D shaft design, subjected to torsional loads, impeller weights, and balance disk forces using SolidWorks Simulation, show the following displacement values: the shaft made of AISI 4140 material experienced a displacement of 0.453 mm. In contrast, the shaft made of AISI 316 material exhibited a displacement of 0.480 mm. The shaft made of AISI 304 material demonstrated the highest displacement at 0.489 mm. The visual representation of these displacements is illustrated in Figure 8.

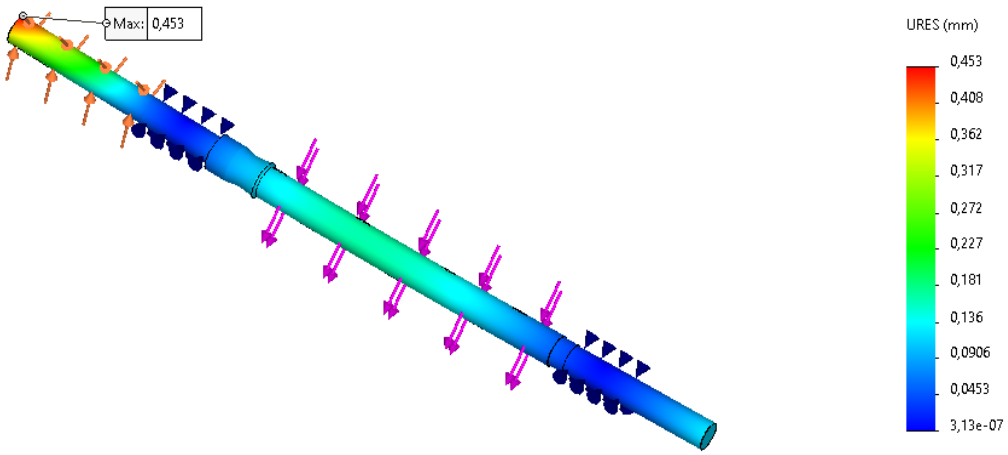

(a)

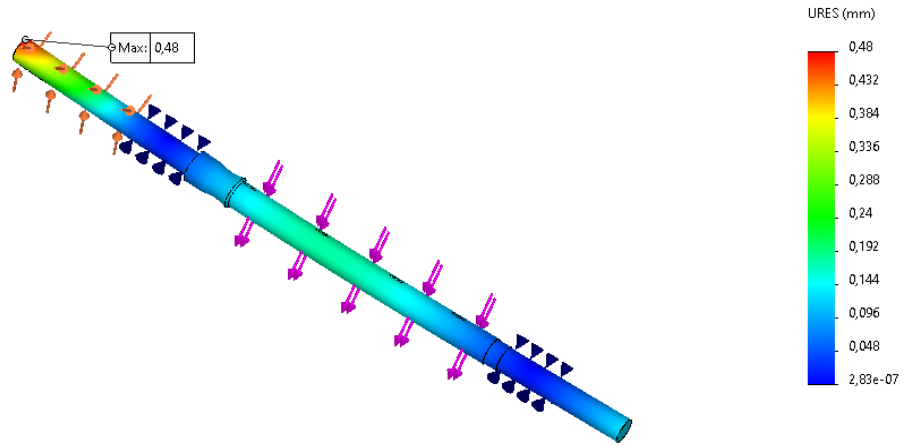

(b)

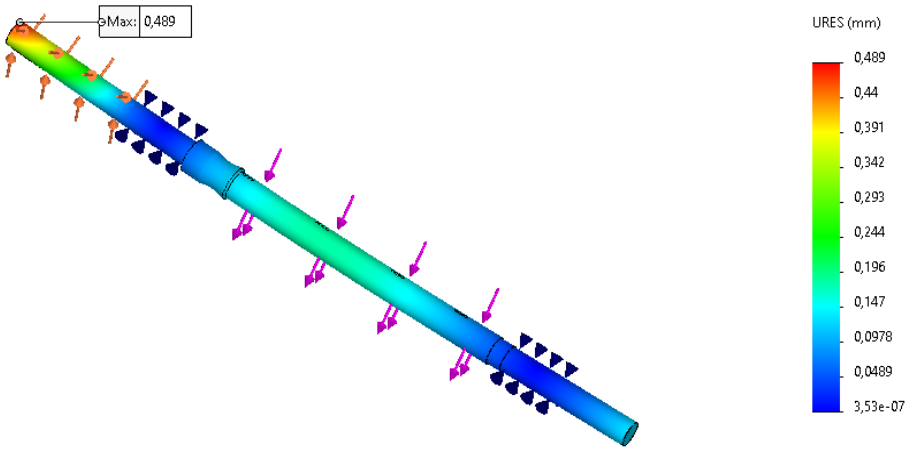

(c)

Figure 8: Displacement value of shaft (a) Material 4140 (b) Material 316 (c) Material 304

3.1.3 Strain

The results of the static strain simulations conducted on the 3D shaft design, which involved applying torsional loads, impeller weights, and balance disk forces using SolidWorks Simulation, reveal the following maximum strain values: the shaft with AISI 4140 material exhibited a maximum strain of 0.000649. Conversely, the shaft with AISI 316 material showed a maximum strain of 0.000679. The shaft made of AISI 304 material experienced the highest maximum strain at 0.000701. The visualization of these strains occurring in the shaft is depicted in Figure 9.

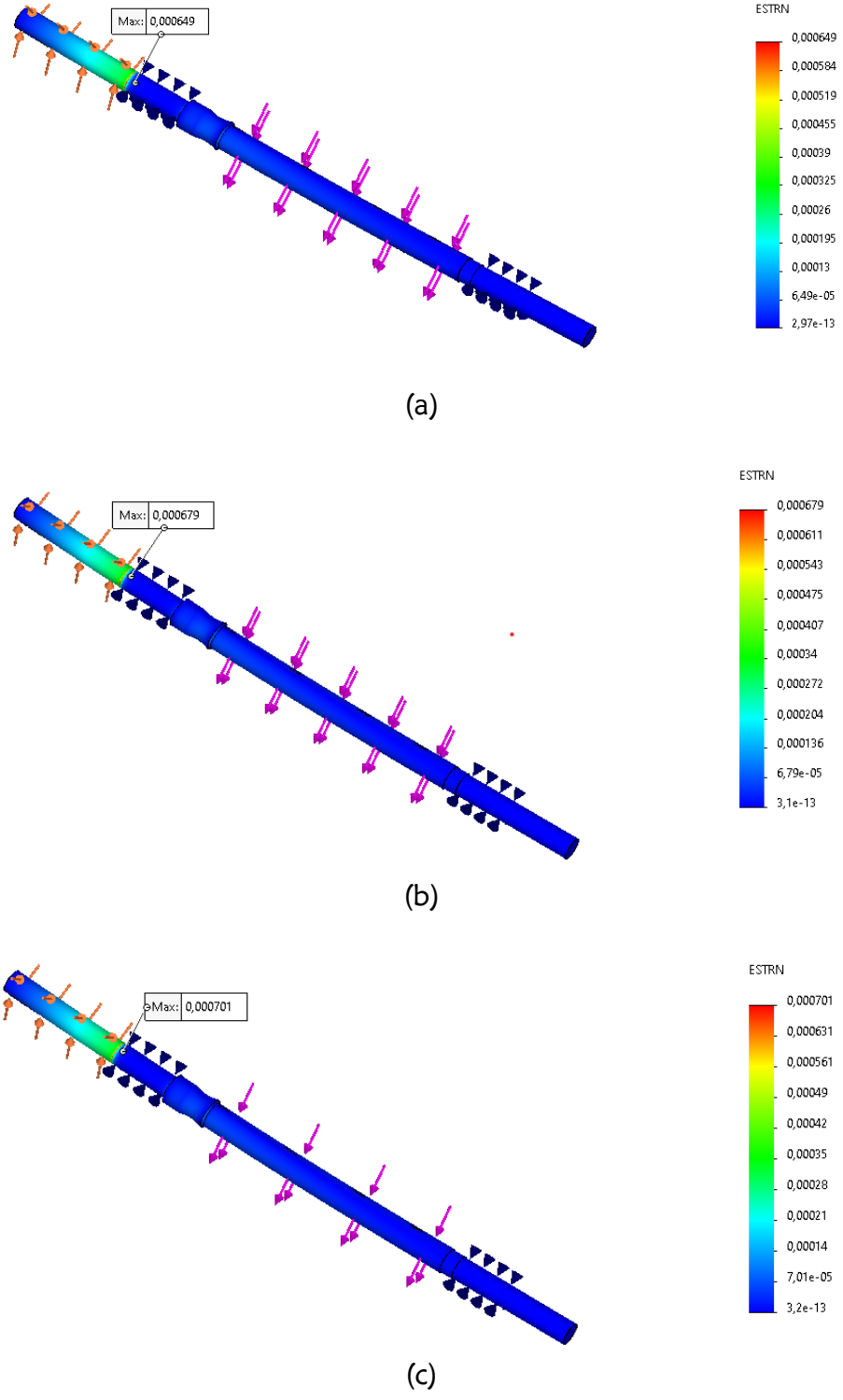

Figure 9: Strain value of shaft (a) Material 4140 (b) Material 316 (c) Material 304

3.1.4 Factor of safety

The results of the safety factor analysis from the static simulations performed on the 3D shaft design, which included torsional loads, impeller weights, and balance disk forces

using SolidWorks Simulation, indicate the following safety factors: the shaft model with AISI 4140 material has a safety factor of 2.7, the shaft with AISI 316 material has a safety factor of 0.9, and the shaft with AISI 304 material has a safety factor of 1.1. This suggests that the 3D shaft design with AISI 4140 material offers the highest safety factor, as the required safety factor for a structure to withstand dynamic loads is typically 2-3 [31]. The visualization of these safety factors in the shaft is shown in Figure 10.

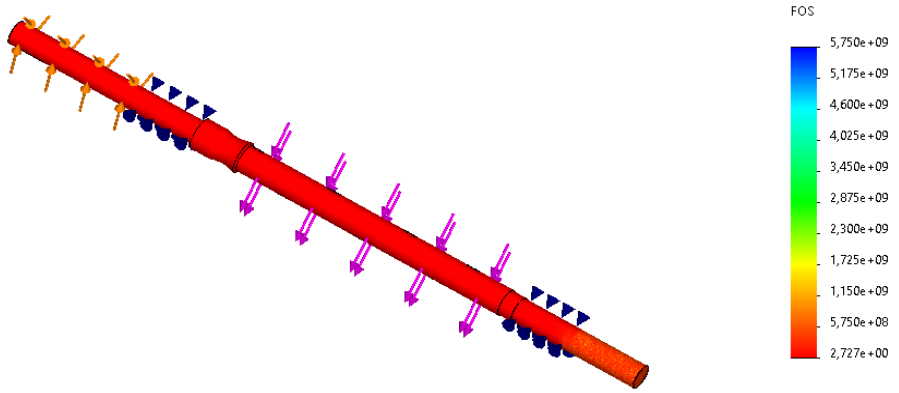

(a)

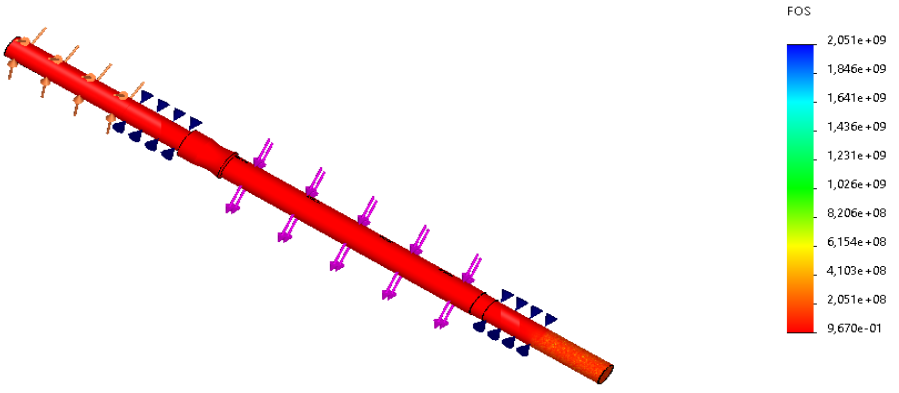

(b)

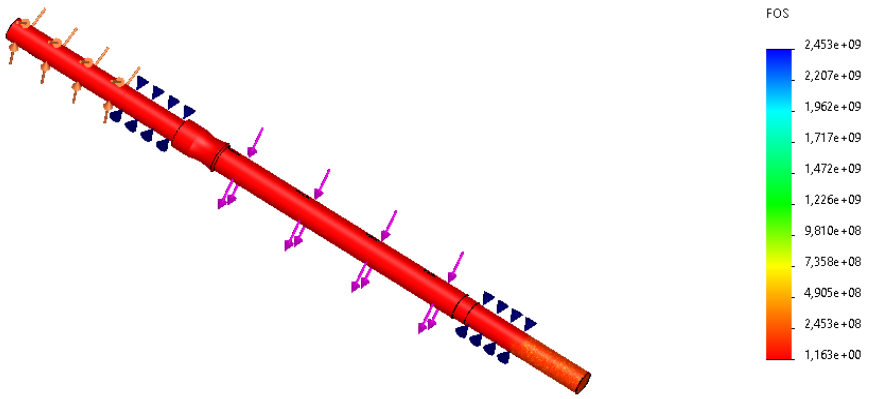

(c)

Figure 10: Value of shaft factor of safety (a) Material 4140 (b) Material 316 (c) Material 304

3.2 Fatigue simulation

Fatigue is typically the most common cause of failure in pump shafts. The initiation of fatigue cracks is a prevalent controlling factor in the lifespan of most small shafts, with surface imperfections being particularly significant [32]. Fatigue accounts for up to 90% of metal failures [33]. Damage resulting from cyclic loading is termed fatigue failure. This type of failure usually occurs after prolonged usage. The fatigue failure mechanism has three phases: crack initiation, propagation, and final fracture [34].

3.2.1 Damage

The maximum damage percentage obtained from the fatigue simulation, conducted using SolidWorks software with an input of 10^6 cycles applied to the 3D shaft model, is illustrated in Figures 11, 12, and 13. The simulation results indicate that the maximum damage percentage for the shaft designed with AISI 4140 material is 38.1%, with damage localized in areas marked in red. This visualization is presented in Figure 11.

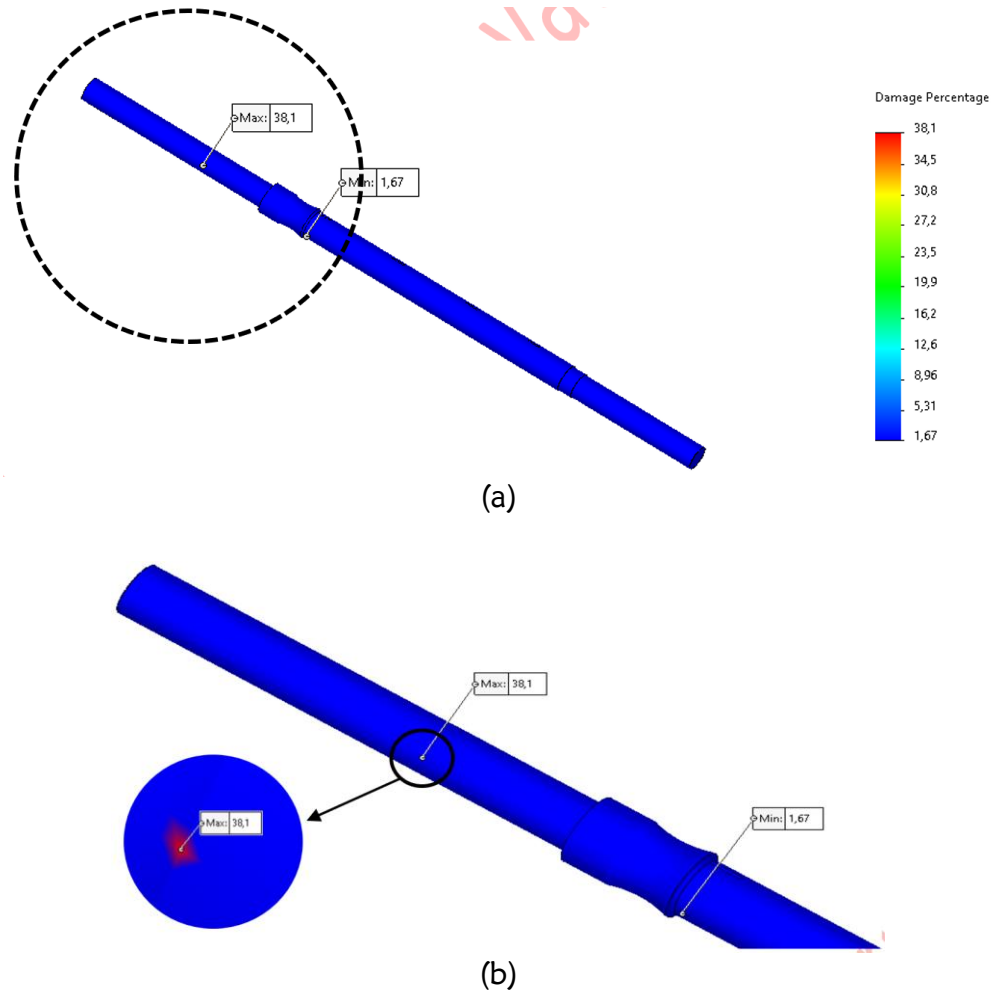

Figure 11: (a) Damage percentage of AISI 4140 material and (b) simulation results of magnification

Figure 12 displays the maximum damage percentage obtained from the fatigue simulation using SolidWorks software on the 3D shaft model with AISI 316 material. The simulation results indicate a maximum damage value of 40.7%, with damage localized in areas highlighted in red.

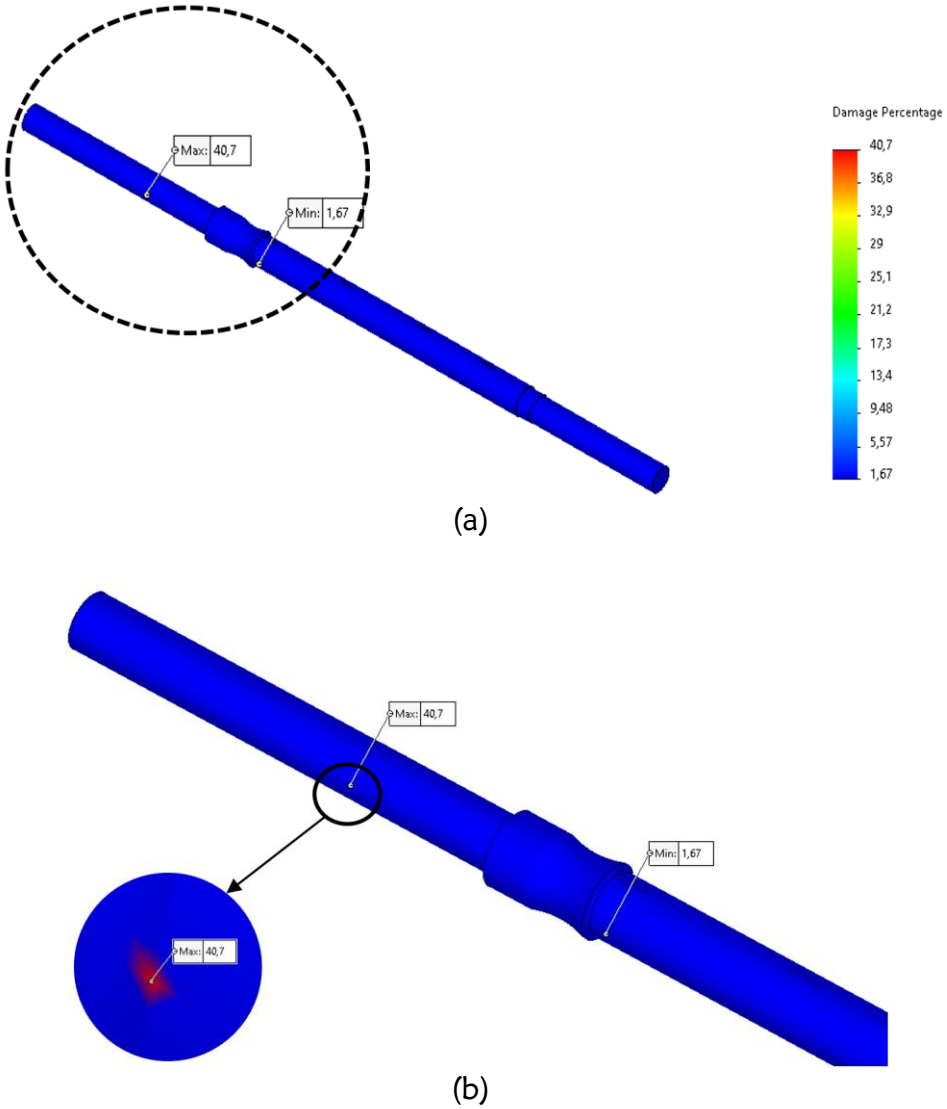

Figure 12: Damage percentage of AISI 316 material (a) simulation results and (b) magnification

Figure 13 illustrates the maximum damage percentage obtained from the fatigue simulation using SolidWorks software on the 3D shaft model with AISI 304 material. The results indicate a maximum damage value of 38.3%, with the damage prominently visible in the areas marked in red in Figure 13.

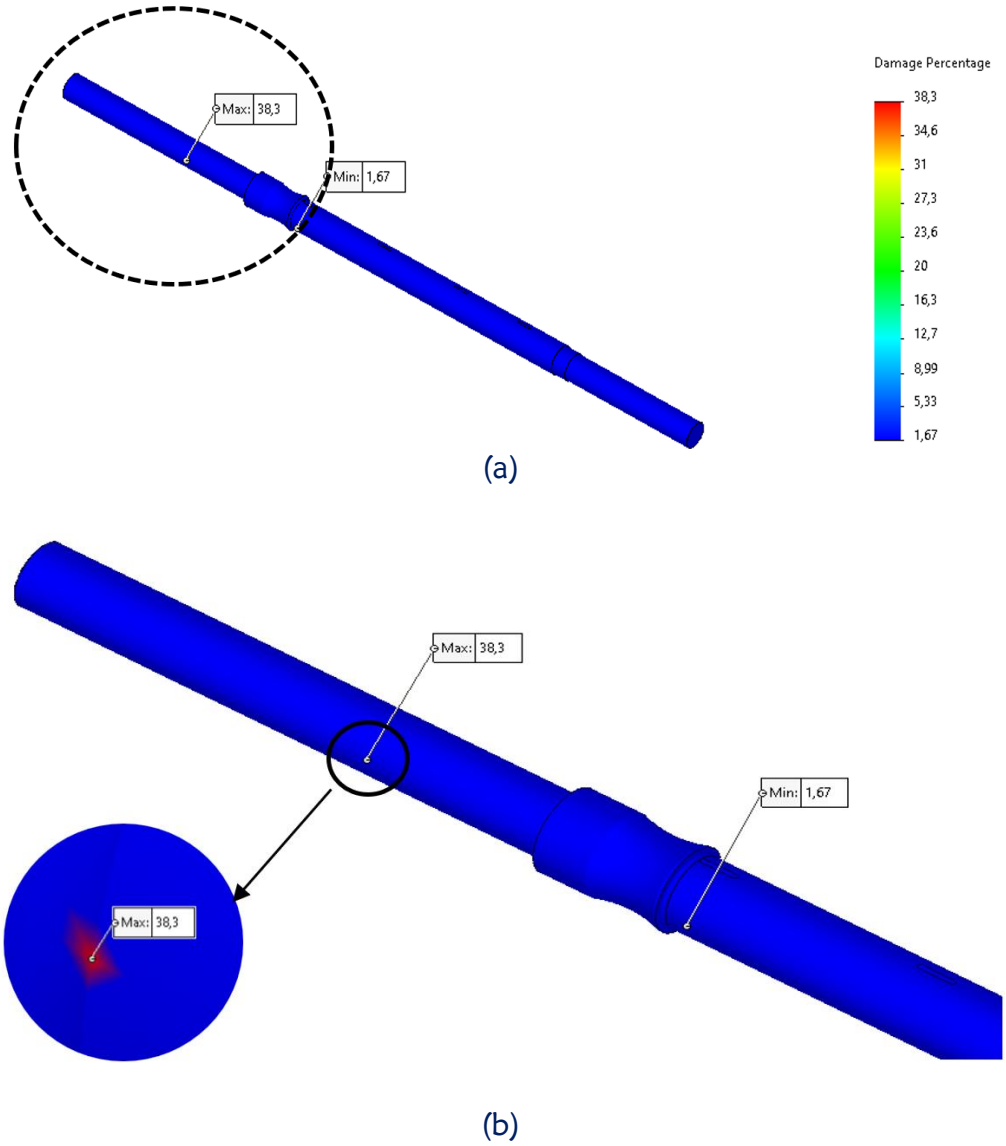

Figure 13: (a) Damage percentage material AISI 304, and Simulation result of magnification of figure a

3.2.2 Usage life

The results of the fatigue life simulation using SolidWorks software with an input of 10^6 cycles applied to the 3D shaft model are illustrated in Figure 14. For the shaft material AISI 4140, the minimum fatigue life was determined to be 2.623×10^6 cycles. This value is depicted in Figure 14, with the minimum life areas highlighted in red in both Figure 14a and the enlarged view in Figure 14b.

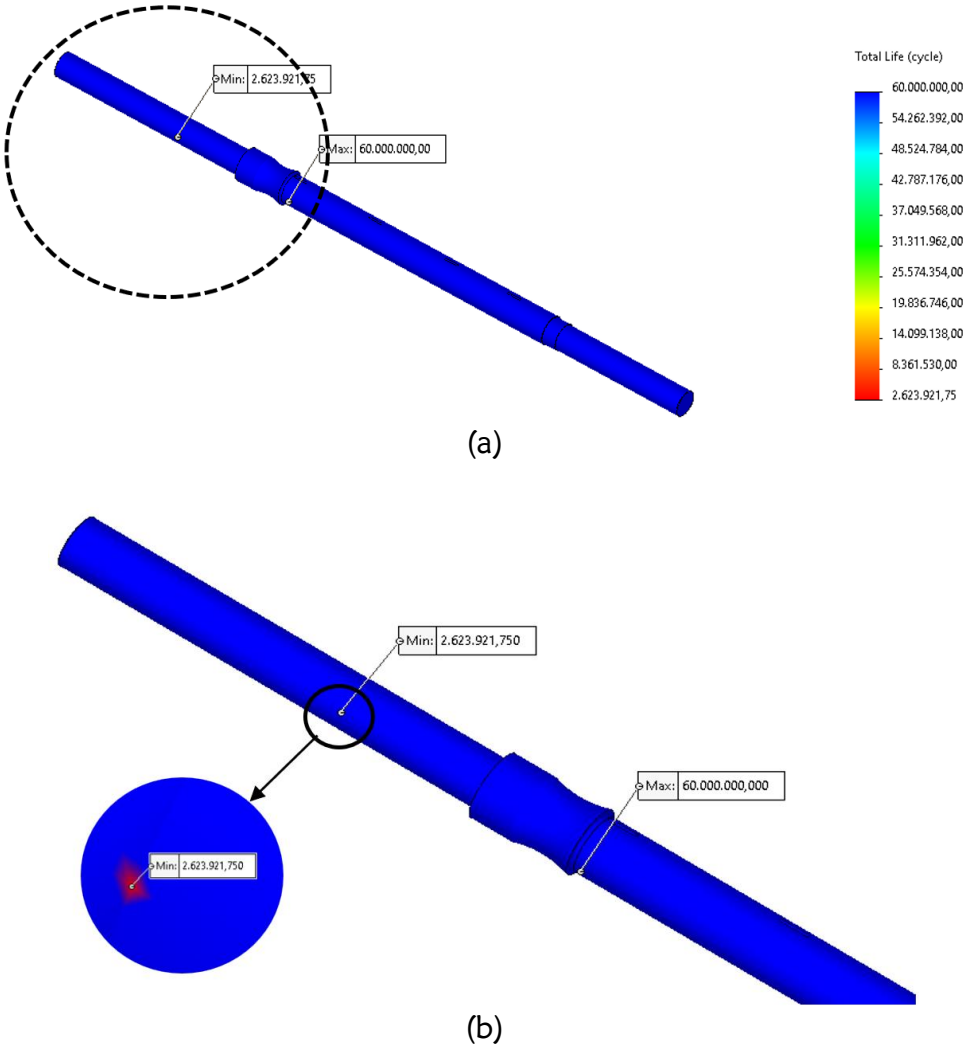

Figure 14: Life of AISI 4140 material (a) simulation result (b) magnification of figure a

The results of the fatigue simulation conducted using SolidWorks software on the shaft made of AISI 316 material are presented in Figure 15. This figure illustrates the fatigue life of the shaft, highlighting the performance and durability metrics based on the simulation data.

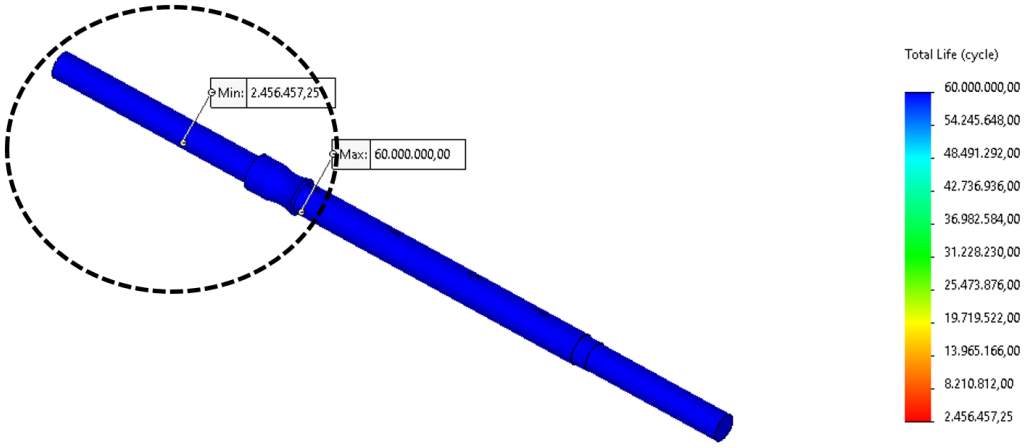

(a)

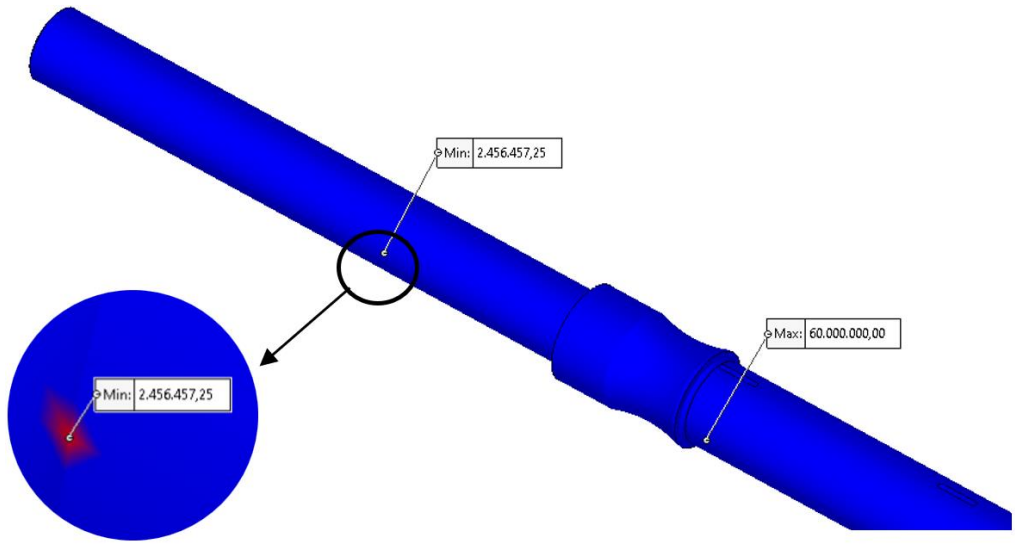

(b)

Figure 15: Life of AISI 316 material (a) simulation result (b) magnification of figure a

Based on Figure 16, the minimum fatigue life obtained is 2.456 × 10^6 cycles. This value is highlighted in Figure 16, with the minimum life areas shown in red. The detailed view is provided in Figure 16a and further enlarged in Figure 16b, illustrating the regions where the minimum life occurs.

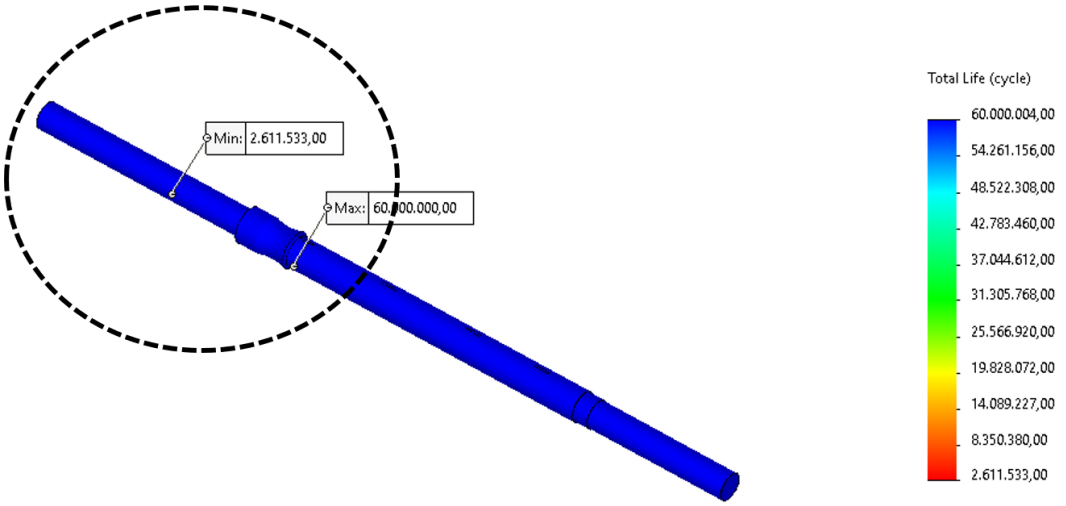

(a)

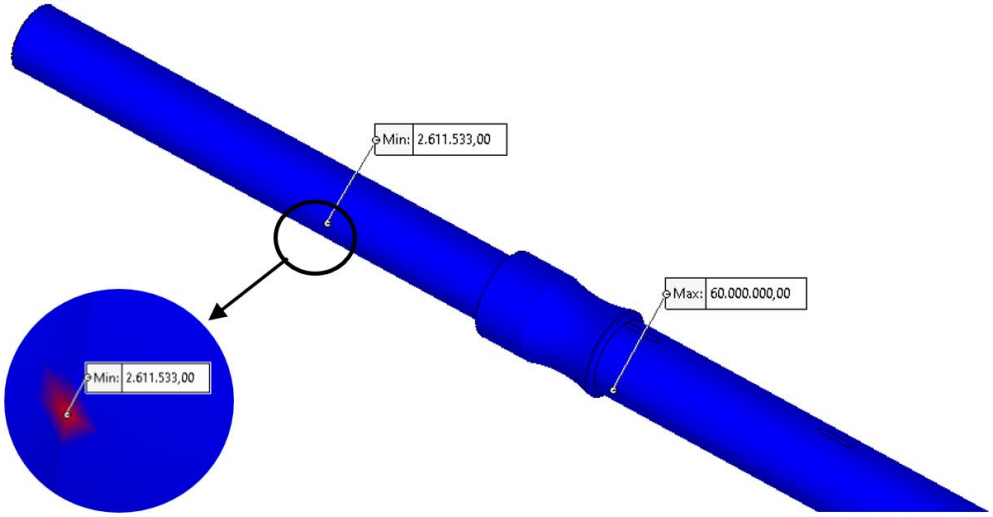

(b)

Figure 16: Life of AISI 304 material (a) simulation result (b) magnification of figure a

Table 2: A Recapitulation of the shaft design model of simulation results

Material	AISI 4140		AISI 316		AISI 304	
	Min	Max	Min	Max	Min	Max
Total Mass (Kg)	43.8		44.7		44.7	
Von Mises Stress	8.44E-08	178	8.40E-08	178	8.43E-08	178
Displacement (mm)	3.31E-07	0.453	2.83E-07	0.48	3.53E-7	0.489
Strain	2.97E-13	0.000649	3.75E-13	0,000679	3.03E-13	0.000701
Safety Factor	2.72		0.96		1.16	

Figure 16 illustrates the results of the fatigue simulation conducted using SolidWorks software on the shaft made of AISI 304 material. The minimum fatigue life obtained is 2.611 × 10^6 cycles. This value is depicted in Figure 16, with the minimum life regions

highlighted in red. The detailed visualization is shown in Figure 16a and further enlarged in Figure 16b, clearly identifying the areas where the minimum life is observed.

4. Constribution and limitations

This study contributes to the field of engineering by providing a comprehensive comparative analysis of three materials—AISI 4140, AISI 316, and AISI 304—for shaft design in multistage centrifugal pumps, precisely Boiler Feed Pumps (BFPs). The research utilizes computer-aided engineering (CAE) simulation through SolidWorks to assess these materials' static and fatigue performance under various loading conditions. By examining parameters such as Von Mises stress, displacement, strain, and safety factor, the study identifies AISI 4140 as the optimal material for shafts in demanding engineering applications due to its superior strength and safety factor. The findings provide valuable insights for engineers and manufacturers in selecting materials that balance mechanical properties and operational longevity in industrial environments. Moreover, the study's methodology, which integrates static and fatigue simulations, serves as a reference for future research aiming to optimize the performance and durability of mechanical components in fluid machinery.

Despite its contributions, this study has several limitations. First, the simulations conducted are based on idealized conditions that may not fully capture the complexities and variabilities of real-world environments. For example, the simulations did not consider temperature fluctuations, corrosion, and unpredictable mechanical wear. Second, the study is limited to three types of materials, which restricts the generalizability of the findings to other potential materials that could be used for shaft design. Furthermore, the mesh independence test results, although indicative of optimal mesh density, still depend on the chosen software and specific settings, which might not be universally applicable. Lastly, the simulations were performed with a fixed number of cycles (10^6 cycles), which may not reflect the actual lifespan of the shaft under varying operational conditions, thereby limiting the understanding of long-term performance.

5. Conclusion and recommendations

This study was conducted to examine and provide an overview of the impact of loads applied to a shaft and its service life after undergoing fatigue testing. The analysis was performed using the finite element method with SolidWorks 2022 software. The simulation results for the AISI 4140 shaft material indicated a maximum stress value of 178 MPa, maximum displacement of 0.453 mm, maximum strain of 0.000649, safety factor of 2.7, maximum damage percentage of 38.1%, and a minimum life of 2,623,921 cycles. For the AISI 316 shaft material, the results showed a maximum stress value of 178 MPa, maximum displacement of 0.48 mm, maximum strain of 0.000679, safety factor of 0.96, maximum damage percentage of 40.7%, and a minimum life of 2,456,457 cycles. Meanwhile, the AISI 304 shaft material recorded a maximum stress value of 178

MPa, maximum displacement of 0.489 mm, strain of 0.000701, safety factor of 1.16, maximum damage percentage of 38.3%, and a minimum life of 2,611,533 cycles. Based on these findings, the AISI 4140 material outperforms the others with a safety factor of 2.7, indicating that it is more durable than AISI 316 and AISI 304 materials. A higher durability of the shaft material reduces the risk of potential failures.

Future studies should address these limitations by incorporating more complex simulation conditions that reflect real-world operating environments, including thermal expansion, corrosion resistance, and varying load conditions. Expanding the range of materials examined, including advanced composites or alloys, could provide a broader perspective on material selection for BFP shafts. Validating the simulation results with experimental testing is also recommended to enhance the reliability of the findings and ensure they apply to actual engineering practices. Furthermore, adopting multi-objective optimization techniques could help identify the best material for mechanical strength and consider cost-efficiency, manufacturability, and environmental impact. Ultimately, future research could explore using different software tools and advanced simulation techniques to cross-validate the results and improve the conclusions' robustness.

Acknowledgements

The authors would like to thank the entire research team at the Machine Construction Laboratory, Universitas Negeri Padang for their input and suggestions during the research implementation.

Declarations

Author contribution

Muhammad Athar Altarisi: Writing – review & editing, Writing – original draft, Conceptualization, Data curation, Formal analysis, Software, Visualization. Rifelino: Writing – review & editing, Methodology, Formal analysis, Software, Supervision. Delima Yanti Sari: Writing – review & editing, Conceptualization, Data curation, Resources, Validation. Wanda Afnison: Writing – review & editing, Formal analysis, Resources, Software, Validation.

Funding statement

This research received no specific grant from any funding agency in the public, commercial, or not-for-profit sectors.

Conflict of interest

The authors declare no conflict of interest in this research and publication.

Ethical Clearance

This research does not involve human subjects.

References

[1] D. Y. S. Low, P. E. Poh, and S. Y. Tang, "Assessing the impact of augmented reality application on students' learning motivation in chemical engineering," *Education for Chemical Engineers*, vol. 39, pp. 31–43, 2022, https://doi.org/10.1016/j.ece.2022.02.004

[2] R. M. Perissinotto *et al.*, "Flow visualization in centrifugal pumps: A review of methods and experimental studies," *J Pet Sci Eng*, vol. 203, p. 108582, 2021, https://doi.org/10.1016/j.petrol.2021.108582

[3] T. Aprianti *et al.*, "A comparison of ground and air source heat pump performance for domestic applications: A case study in Perth, Australia," *Teknomekanik*, vol. 4, no. 2, pp. 55–63, 2021, https://doi.org/10.1002/er.7133

[4] G. Yang, X. Zhao, D. Zhang, L. Geng, X. Yang, and X. Gao, "Hydraulic components' matching optimization design and entropy production analysis in a large vertical centrifugal pump," *Journal of Mechanical Science and Technology*, vol. 35, no. 11, pp. 5033–5048, 2021, https://doi.org/10.1007/s12206-021-1021-2

[5] X. Li, B. Chen, X. Luo, and Z. Zhu, "Effects of flow pattern on hydraulic performance and energy conversion characterisation in a centrifugal pump," *Renew Energy*, vol. 151, pp. 475–487, 2020, https://doi.org/10.1016/j.renene.2019.11.049

[6] B. R. Rode and R. Khare, "A review on development in design of multistage centrifugal pump," *Advances in Computational Design*, vol. 6, no. 1, pp. 43–53, 2021, https://doi.org/10.12989/acd.2021.6.1.43

[7] S. Selimli and S. Sunay, "Feasibility study of the energy and economic gain that can be achieved by driving the boiler feedwater pump with a backpressure steam turbine," *Proceedings of the Institution of Mechanical Engineers, Part A: Journal of Power and Energy*, vol. 235, no. 5, pp. 1254–1266, 2021, https://doi.org/10.1177/0957650920969466

[8] W. Safira Rahmania, H. Elvian Gayuh Prasetya, and F. Hesty Sholihah, "Maintenance analysis of boiler feed pump turbine using failure mode effect analysis (fmea) methods," in *International Electronics Symposium: The Role of Autonomous and Intelligent Systems for Human Life and Comfort*, 2020, pp. 54–59. https://doi.org/10.1109/IES50839.2020.9231886

[9] M. Moleda, A. Momot, and D. Mrozek, "Predictive maintenance of boiler feed water pumps using SCADA data," *Sensors (Switzerland)*, vol. 20, no. 2, pp. 1–19, 2020, https://doi.org/10.3390/s20020571

[10] B. Ghorbani, S. Zendehboudi, and M. Moradi, "Development of an integrated structure of hydrogen and oxygen liquefaction cycle using wind turbines, Kalina

power generation cycle, and electrolyzer," *Energy*, vol. 221, p. 119653, 2021, https://doi.org/10.1016/j.energy.2020.119653

[11] S. O. Oyedepo *et al.*, "Thermodynamics analysis and performance optimization of a reheat – Regenerative steam turbine power plant with feed water heaters," *Fuel*, vol. 280, no. July, p. 118577, 2020, https://doi.org/10.1016/j.fuel.2020.118577

[12] R. A. Ufa, Y. Y. Malkova, V. E. Rudnik, M. V. Andreev, and V. A. Borisov, "A review on distributed generation impacts on electric power system," *Int J Hydrogen Energy*, vol. 47, no. 47, pp. 20347–20361, 2022, https://doi.org/10.1016/j.ijhydene.2022.04.142

[13] N. Kumar, R. Kumar, B. K. Sarkar, and S. Maity, "Condition monitoring of hydraulic transmission system with variable displacement axial piston pump and fixed displacement motor," *Mater Today Proc*, vol. 46, pp. 9758–9765, 2019, https://doi.org/10.1016/j.matpr.2020.09.327

[14] Q. Li, S. Abdullah, and M. R. M. Rasani, "A Review of Progress and Hydrodynamic Design of Integrated Motor Pump-Jet Propulsion," *Applied Sciences (Switzerland)*, vol. 12, no. 8, pp. 1–29, 2022, https://doi.org/10.3390/app12083824

[15] N. Hou *et al.*, "Failure modes, mechanisms and causes of shafts in mechanical equipment," *Eng Fail Anal*, vol. 136, no. February, p. 106216, 2022, https://doi.org/10.1016/j.engfailanal.2022.106216

[16] A. Shokri and M. Sanavi Fard, "Principles, operational challenges, and perspectives in boiler feedwater treatment process," *Environmental Advances*, vol. 13, no. April, p. 100389, 2023, https://doi.org/10.1016/j.envadv.2023.100389

[17] Y. Li, X. Zhao, Z. Liu, and X. Sun, "Vibration fault detection method of boiler feed pump based on Hilbert vibration decomposition," *International Journal of Manufacturing Technology and Management*, vol. 37, no. 3–4, pp. 334–348, 2023, https://doi.org/10.1504/IJMTM.2023.133474

[18] X. Liu, D. Xu, J. Lin, L. Zhang, Y. Zeng, and Q. Chen, "Failure analysis and factors influencing spline wear in hydraulic motors of charging pumps in nuclear power plants," *Eng Fail Anal*, vol. 156, p. 107780, 2024, https://doi.org/10.1016/j.engfailanal.2023.107780

[19] D. van Tonder, "Boiler feed pump low load – leak off recirculation study," Faculty of Engineering and the Built Environment, 2020.

[20] Y. Xiao, Z. Sun, G. Sun, and L. Wan, "Numerical study on dynamic response of double drive shafts of dual-coupled axial piston pump under various load ratios," *Eng Fail Anal*, vol. 163, p. 108558, 2024, https://doi.org/10.1016/j.engfailanal.2024.108558

[21] M. A. Sabtu, A. E. Admi, M. Mohamed, S. A. Osman, and S. A. Osman, "Finite Element Analysis of Stress Distribution in AL6061 Frame Structures Under Varying Applied Loads," *International Journal of Integrated Engineering (IJIE)*, vol. 16, no. 2, pp. 259–269, 2024, https://doi.org/10.30880/ijie.2024.16.02.027

[22] S. Bidari, M. Kamyab, H. Ghandhari, and A. Komeili, "Efficacy of Computer-Aided Design and Manufacturing Versus Computer-Aided Design and Finite Element Modeling Technologies in Brace Management of Idiopathic Scoliosis: A Narrative Review," *Asian Spine J*, vol. 15, no. 2, pp. 271–282, 2021, https://doi.org/10.31616/asj.2019.0263

[23] I. Daniyan, K. Mpofu, L. Daniyan, F. Fameso, and M. Oyesola, "Computer aided simulation and performance evaluation of additive manufacturing technology for component parts manufacturing," *International Journal of Advanced Manufacturing Technology*, vol. 107, no. 11–12, pp. 4517–4530, 2020, https://doi.org/10.1007/s00170-020-05340-8

[24] W. Jarrett, S. P. Jeffs, F. Korkees, and M. Rawson, "The opportunities and challenges of hybrid composite driveshafts and their couplings in the aerospace industry: A review," *Compos Struct*, vol. 320, no. June, p. 117203, 2023, https://doi.org/10.1016/j.compstruct.2023.117203

[25] B. Regassa Hunde and A. Debebe Woldeyohannes, "Future prospects of computer-aided design (CAD) – A review from the perspective of artificial intelligence (AI), extended reality, and 3D printing," *Results in Engineering*, vol. 14, no. June, p. 100478, 2022, https://doi.org/10.1016/j.rineng.2022.100478

[26] M. N. Mastrone and F. Concli, "CFD simulations of gearboxes: implementation of a mesh clustering algorithm for efficient simulations of complex system' s architectures," *International Journal of Mechanical and Materials Engineering*, vol. 16, no. 1, pp. 1–19, 2021, https://doi.org/10.1186/s40712-021-00134-6

[27] I. Romanenko, Y. Martseniuk, and O. Bilohub, "Modeling the Meshing Procedure of the External Gear Fuel Pump Using a CFD Tool," *Computation*, vol. 10, no. 7, pp. 1–19, 2022, https://doi.org/10.3390/computation10070114

[28] A. Volk, U. Ghia, and G. R. Liu, "Assessment of CFD-DEM solution error against computational cell size for flows through a fixed-bed of binary-sized particles," *Powder Technol*, vol. 325, pp. 519–529, 2018, https://doi.org/10.1016/j.powtec.2017.11.051

[29] Z. Xie *et al.*, "Effect of cell size on erosion representation and recommended practices in CFD," *Powder Technol*, vol. 389, pp. 522–535, 2021, https://doi.org/10.1016/j.powtec.2021.05.066

[30] M. Isiet, I. Mišković, and S. Mišković, "Review of peridynamic modelling of material failure and damage due to impact," *Int J Impact Eng*, vol. 147, p. 103740, 2021, https://doi.org/10.1016/j.ijimpeng.2020.103740

[31] G. L. Arumparithy, R. Adalarasan, M. Santhanakumar, and L. Mulugeta, " Parameter Design in Carbonitriding of EN36, 16MnCr5, and AISI 4140 Steels Using Principal Component-Based Grey Incidence (PGI)," *Advances in Materials Science and Engineering*, pp. 1–12, 2022, https://doi.org/10.1155/2022/8138198

[32] N. Hou *et al.*, "Failure modes, mechanisms and causes of shafts in mechanical equipment," *Eng Fail Anal*, vol. 136, p. 106216, 2022, https://doi.org/10.1016/j.engfailanal.2022.106216

[33] P. Foti, N. Razavi, A. Fatemi, and F. Berto, "Multiaxial fatigue of additively manufactured metallic components: A review of the failure mechanisms and fatigue life prediction methodologies," *Prog Mater Sci*, vol. 137, p. 101126, 2023, https://doi.org/10.1016/j.pmatsci.2023.101126

[34] K. Tang, Z. Du, P. Ferro, and F. Berto, "Crack initiation and propagation from geometric microdefects: Experiment and transition fatigue behavior," *Fatigue Fract Eng Mater Struct*, vol. 44, no. 9, pp. 2323–2336, 2021, https://doi.org/10.1111/ffe.13492

Nomenclature

W = Weight Force (N)
m = mass (kg)
g = Earth's gravity (m/s^2)
τ = Moment of Force (Torque) (Nm)
P = Power (W)
ω = Angular velocity (rad/s)